



Development of a series of 3-hydroxyquinolin-2(1H)-ones as selective inhibitors of HIV-1 reverse transcriptase associated RNase H activity

Virginie Suchaud^{a,b}, Fabrice Bailly^{a,b,*}, Cédric Lion^{a,b}, Enzo Tramontano^c, Francesca Esposito^c, Angela Corona^c, Frauke Christ^d, Zeger Debyser^d, Philippe Cotellet^{a,b}

^a Université Lille Nord de France, F-59000 Lille, France

^b USTL, EA 4478 Chimie Moléculaire et Formulation, F-59655 Villeneuve d'Ascq, France

^c Department of Life and Environmental Sciences, University of Cagliari, Cittadella Universitaria di Monserrato SS554, 09042 Monserrato (Cagliari), Italy

^d Molecular Medicine, K. U. Leuven and IRC KULAK, Kapucijnenvoer 33, B-3000 Leuven, Flanders, Belgium

ARTICLE INFO

Article history:

Received 2 March 2012

Revised 17 April 2012

Accepted 20 April 2012

Available online 30 April 2012

Keywords:

3-Hydroxyquinolin-2(1H)-one

Ribonuclease H

Magnesium complexation

Antiretroviral

ABSTRACT

We report herein the synthesis of a series of 3-hydroxyquinolin-2(1H)-one derivatives. Esters and amide groups were introduced at position 4 of the basis scaffold and some modulations of the benzenic moiety were performed. Most compounds presented selective inhibitory properties in the 10–20 μ M range against HIV-1 reverse transcriptase associated ribonuclease H activity, without affecting the integrase and reverse transcriptase DNA polymerase activities. Unfortunately all tested compounds exhibited high cellular cytotoxicity in cell culture which limited their applications as antiviral agents.

© 2012 Elsevier Ltd. All rights reserved.

Since the discovery of the human immunodeficiency virus (HIV) 28 years ago, the progress made toward developing effective anti-HIV therapies has superseded that of any other antiviral drug discovery initiative. Highly active antiretroviral therapies (HAART) combining several drugs have shown effectiveness and moved the prognosis of HIV patients from that of high morbidity and mortality to, for many at least, a chronic, manageable but still complex disease.^{1,2} However, this type of treatment has important limitations such as cost, patient's observance, occurrence of various side effects due to drug toxicity and, most importantly, loss of activity due to the development of multidrug and cross resistance.^{3,4} In order to minimize the appearance of such multiple resistant strains, novel classes of HIV drugs are therefore needed.

In this regard, there has been considerable interest in the ribonuclease H (RNase H) function associated to the viral coded reverse transcriptase (RT), as an attractive alternative target that may lead to the next generation of anti-HIV drug. A few classes of RT RNase H inhibitors have been identified in the recent years.^{5,6} Whereas some may bind allosterically to a different site, these compounds mainly interact with the magnesium metal cofactors within the catalytic core of the enzyme. In particular, because of the structural and functional similarities of the catalytic cores of HIV-1 integrase

(HIV-1 IN) and the RT RNase H function, compounds inhibiting both activities have already been reported.⁷

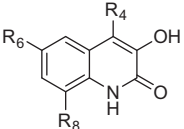
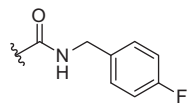
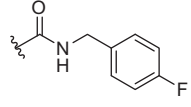
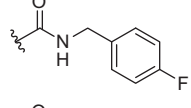
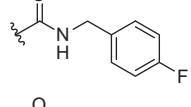
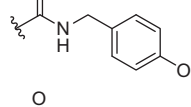
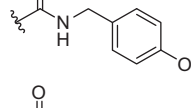
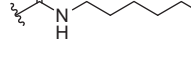
In order to target the catalytic site of the RT RNase H function, we decided to focus our attention on the 3-hydroxyquinolin-2(1H)-one scaffold for several reasons. It was indeed shown to complex some bivalent metals,⁸ and by introducing a carbonyl function at position 4 this scaffold comprises three oxygens, the topology of which appears ideal to bind two divalent cations separated by 4–5 Å in the case of an enzyme–metals–ligand ternary complex. Such a pharmacophore can be observed in the structure of most recently discovered RNase H inhibitors. We report herein the preparation of a series of substituted 3-hydroxyquinolin-2(1H)-ones. The inhibitory properties of all synthesized compounds were evaluated against RT associated RNase H and polymerase functions, together with integrase. Their physico-chemical properties regarding magnesium chelation were also studied, and antiviral activities were investigated. Additionally, an *in silico* molecular docking method for RT RNase H binding was developed in order to assess the ability of our molecules to fit in the RNase H active site.

A series of nineteen 3-hydroxy-2-oxoquinoline-4-carboxylic acids (**3a–e**), ethyl 3-hydroxy-2-oxoquinoline-4-carboxylates (**2a–f**) and 3-hydroxy-2-oxoquinoline-4-carboxamides (**4a–g**) mostly substituted at positions 6 and 8 of the quinoline moiety was elaborated (Table 1). Esters **2a–e** were prepared and used as versatile precursors of the acids, amides and decarboxylated compounds. Commercial substituted isatins were thus reacted with

* Corresponding author. Tel.: +33 320 33 72 31; fax: +33 320 33 63 09.

E-mail address: fabrice.bailly@univ-lille1.fr (F. Bailly).

Table 1
Biological activities of the 3-hydroxyquinolin-2(1H)-one derivatives

	R ⁴	R ⁶	R ⁸	IC ₅₀ (μM) RT RNase H ^a	EC ₅₀ ^c (μM)	CC ₅₀ ^d (μM)	IC ₅₀ (μM)	
							HIV-1 RT polymerase ^e	HIV-1 IN ^f
5a	H	H	H	>100 (97%) ^b	>115	115	—	—
3a	—CO ₂ H	H	H	59	>250	>250	—	—
3b	—CO ₂ H	NO ₂	H	97	>250	>250	—	—
3c	—CO ₂ H	Cl	H	>100 (100%)	>250	>250	—	—
3d	—CO ₂ H	F	H	>100 (100%)	>250	250	—	—
3e	—CO ₂ H	H	F	>100 (88%)	>250	>250	—	—
2a	—CO ₂ Et	H	H	16	>210	210	—	—
2b	—CO ₂ Et	NO ₂	H	64	>118	118	—	—
2c	—CO ₂ Et	Cl	H	>100 (100%)	>117	117	—	—
2d	—CO ₂ Et	F	H	>100 (100%)	>134	134	—	—
2e	—CO ₂ Et	H	F	>100 (100%)	>238	238	—	—
2f	—CO ₂ Et	NH ₂	H	>100 (100%)	>250	250	—	—
4a		H	H	19	>29	29	>250	>250
4b		Cl	H	18	>28	28	>250	>250
4c		F	H	22	>24	24	>250	>250
4d		H	F	75	>6.8	8	—	—
4e		F	H	19	>29	29	>250	>250
4f		H	F	74	>8	8	—	—
4g		H	F	49	>22	22	—	—
RDS 1643				13				

^a Concentration required to inhibit by 50% the in vitro RT associated RNase H activity.

^b Percentage of enzyme activity measured at 100 μM compound concentration.

^c Effective concentration required to reduce HIV-1-induced cytopathic effect by 50% in MT-4 cells.

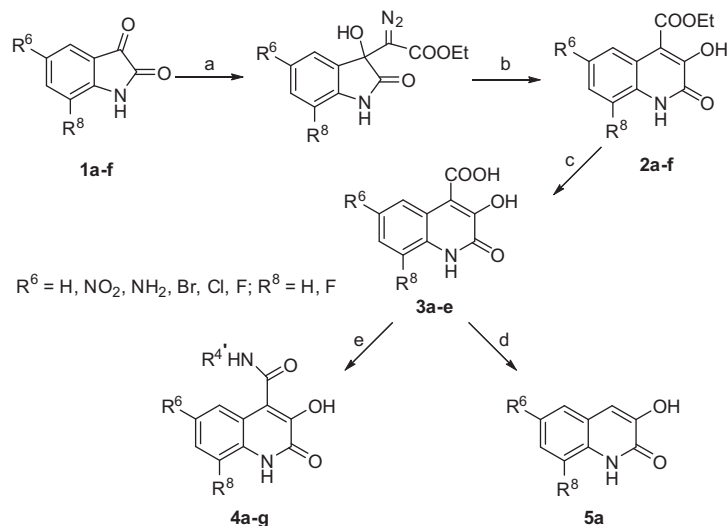
^d Cytotoxic concentration required to reduce MT-4 cell viability by 50%.

^{e,f} Concentration required to inhibit by 50% the in vitro RT associated RNA dependent polymerase and integrase activities, respectively.

ethyl diazoacetate in the presence of diethylamine, and the 3-hydroxyquinolin-2-(1H)-one scaffold was obtained via subsequent Eistert ring expansion of the crude adducts after dilute aqueous acidic treatment, as depicted in Scheme 1.^{9,10} Reduction of **2b** by catalytic hydrogenation yielded amine **2f**. Saponification of esters **2a–e** led to the corresponding carboxylic acid series **3a–e**, and the decarboxylated counterpart **5a** was obtained after prolonged heating of **3a** in basic conditions. The carboxylic acids were then converted into intermediate acid chlorides and submitted to

addition-elimination with the adequate primary amines to afford amides **4a–g**.

Firstly, we investigated the magnesium chelating properties of these compounds. A detailed study using UV spectrophotometry, ¹H NMR and ¹³C NMR spectrometries was carried out on amide **4a**. Its incubation with magnesium acetate provoked large hyperchromic effects in the 240–250 nm and 310–340 nm regions of its UV spectrum. It was very slightly modified in presence of sodium acetate whereas it kept unchanged in presence of



Scheme 1. Reagents and conditions: (a) $\text{N}_2\text{CHCO}_2\text{Et}$, Et_3NH , EtOH, rt, 72 h; (b) aq. 6 M HCl, rt, 2 h; (c) NaOH, EtOH, reflux, 2 h; (d) aq. 2 M NaOH, EtOH, reflux, 12 h; (e) (i) SOCl_2 , AcOEt reflux, 30 min; (ii) $\text{R}_4'\text{NH}_2$, $i\text{Pr}_2\text{EtN}$, rt, 12 h.

magnesium chloride. The Job method of continuous variation was applied in order to determine the stoichiometry of the detected magnesium complexes, and maximum effects were obtained at 330 or 340 nm for ligand volumic fractions of 0.5 and 0.67, evidencing two metal/ligand stoichiometries in solution (1:2 and 1:1). ^1H and ^{13}C NMR experiments gave further insight into the molecular complexation process. Upon addition of magnesium acetate, lowfield shifts variations of 0.20, 1.36 and 0.32 ppm were measured for the cyclic amide proton, the enolic proton and the exocyclic amide proton, respectively. It is noteworthy that magnesium acetate did not induce the deprotonation of the enolic function. The signals for carbons C_2 and C_3 were also largely shifted with deshieldings of 9.7 and 16.4 ppm, respectively. Nearby carbons C_4 (−12.9 ppm), C_{4a} (+4.6 ppm) and C_{8a} (−3.9 ppm) were also significantly affected. According to the formerly determined stoichiometries, we also synthesized two magnesium complexes **4a'** and **4a''** by incubating the amide **4a** with 0.5 and 1.0 equiv of magnesium hydroxide, respectively. The ^1H and ^{13}C NMR spectra of these two isolated solids were strictly identical to those reported above for the complexes formed in situ. The proposed structures according to the elemental analyses data are represented in Figure 1. Unfortunately, the association constants of the magnesium complexes could not be determined in vitro due to irreproducible values.

Table 1 reports the biological data for this series of 3-hydroxyquinolin-2(1H)-ones. Encouraging inhibitory properties were detected on the RT associated RNase H function. The most active compounds were ester **2a** and amides **4a–4c**, and **4e** with IC_{50} values between 16 and 22 μM , close to that of the diketoacid reference compound RDS1643 (IC_{50} = 13 μM).⁷ The substitution of the benzenic ring by nitro (IC_{50} = 64 μM), halogeno and amino functions (IC_{50} > 100 μM) sharply decreased the inhibitory potency of

unsubstituted ester **2a** (IC_{50} = 16 μM). This was also the case in the acid series by comparing the properties of **3a** (IC_{50} = 59 μM) to those of **3b** (IC_{50} = 97 μM) and **3c–e** (IC_{50} > 100 μM). Decarboxylated compound **5a** was devoid of any inhibitory property, indicating that our molecules might indeed bind to the active site via chelation of the two magnesium cofactors by the three-oxygen pharmacophore. The introduction of an amide function at position 4 proved to be advantageous since it led to a reproducible activity of almost the entire series of amides **4a–g**. Among these compounds, the *para*-fluorophenylacetamido (**4a–c**) and *para*-methoxyphenylacetamido (**4e**) groups were particularly favorable for the HIV-1 RNase H inhibition. For these amide derivatives, the measured inhibitory properties proved to be lower for compounds substituted at position 8 by a fluorine atom, which may be due to its electronic effect on the heterocyclic moiety. For instance, there was a fourfold increase of the IC_{50} value upon substitution of compound **4a** (IC_{50} = 19 μM) by a fluorine atom (**4d**, IC_{50} = 75 μM). Finally the antiviral activities of all the compounds in MT-4 cells were evaluated, but this study was unfortunately impaired by the relatively high cytotoxicities.

In order to evaluate the selectivity of this scaffold, the most active compounds **4a–c** and **4e** were also tested against two magnesium-dependent viral enzymes, HIV-1 RT associated RNA dependent DNA polymerase and HIV-1 integrase (Table 1). Interestingly, none of the newly synthesized compounds were able to inhibit the HIV-1 IN activities and RT polymerase at concentrations up to 250 μM (IC_{50} > 250 μM), indicating a selective preference for the RNase H domain. In addition, the ability of compound **4a** to bind to the isolated RNase H domain (p15) was measured to confirm the hypothesis that the 3-hydroxyquinolin-2(1H)-ones might bind to the RNase H active site. In fact, since the RNase H domain contains one tryptophan and six tyrosine residues as intrinsic fluorophores, it has been reported that when the p15 domain is excited at a wavelength of 290 nm the contribution of tryptophan to the fluorescence signal is maximized, whereas the fluorescence energy transfer from the tyrosine residues to the tryptophan residue is minimized. Upon binding of a ligand within its active site, the intrinsic fluorescence of the HIV-1 RT-associated RNase H domain is therefore quenched.¹¹ Importantly, compound **4a** was thus shown to bind into the RNase H catalytic site as it completely quenches the p15 isolated domain intrinsic fluorescence (Fig. 2). As previously described,¹² 2-hydroxy-1,2,3,4-tetrahydroisoquinoline-1,3-dione (HTHI) was used as a positive control.

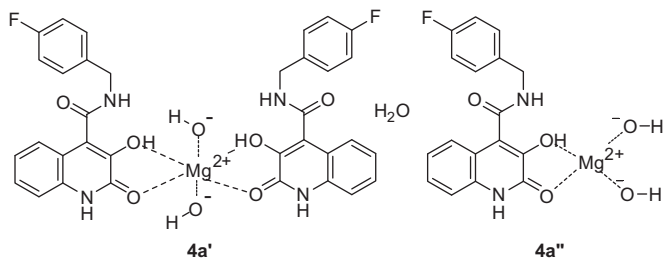


Figure 1. Proposed structures for the isolated complexes **4a'** and **4a''**.

Given the ability of the 4-amido series to inhibit the RT RNase H associated activity by interacting with the RNase H active site, we decided to perform *in silico* docking studies in order to determine a possible binding mode with the target and to propose some pharmacomodulated structures for ligand/protein interactions improvement. To our knowledge, there is only one report of molecular docking on specific RT RNase H inhibition in the literature.¹³ However, this work was carried out on the basis of the crystallographic structure PDB:1RTD,¹⁴ which does not contain an intact and active RNase H domain, and we believe those docking results to be seriously flawed. In this RT complex, Glu478 was indeed mutated into Gln478, precisely to inhibit RNase H activity, while the ligand is bound to the polymerase site. Consequently, the RNase H catalytic site of this crystal structure is not operational: the putative positions of the metal cations greatly differ from that in the active protein and the physico-chemical properties of the cavity are profoundly changed (see [Supplementary data, Fig. 1](#)). After a screening of all available crystal structures, we eventually selected structure PDB:3K2P of the dimerized HIV-1 RT RNase H domain co-crystallized with β -thujaplicinol and two manganese cofactors as the most relevant option for molecular docking. Taking into account the NMR data obtained for the synthesized magnesium complexes of our molecules, we used the enol form for the 4-amido substituted series and the enolate form for the ester series. The docking method was developed using β -thujaplicinol as a template and CHEMPLP was eventually chosen among the various fitness functions available in the CCDC Gold Suite.¹⁵ After validation of the procedure, the statistically relevant highest ranked clusters were examined for amides **4a–g** and ternary complexes were minimized.

As expected, the results confirm the ability of this three oxygen pharmacophore to chelate both metal cofactors within the active site and the putative binding mode is consistent throughout the whole series ([Fig. 3A](#)). In addition to the complexation with both cations, the quinoline scaffold is placed in such a way that the oxygen of the carbonyl at position 2 may also interact with Arg557 through hydrogen bonding, while the lipophilic side chain at position 4 is able to occupy the small hydrophobic pocket created by residues Gln475, Gln500, Tyr501 and Trp535 ([Fig. 3B](#)). In the case of active amides **4a–g** the occupancy of this cavity by the substituent seems to be much better optimized than it is for esters **2a–f** (see [Supplementary data](#)), which may be due to the greater propensity of the aromatic ring to bury itself because of its high lipophilicity. This factor, together with the difference of ligand ionic state observed experimentally in the synthesized complexes, may explain the difference of activity between the amide and ester

series. It is unclear, however, as to why ester **2a** inhibits RNase H activity while the other esters are found to be inactive.

The recent discovery of more potent RT RNase H inhibitors such as pyrimidinol carboxylic acids, *N*-hydroxyquinazolinones or *N*-hydroxynaphthyridinones^{17–19} indicate that lipophilic aromatic side chains may be able to interact favorably either with His539 via π -stacking or occupy a closeby hydrophobic pocket created by residues Asn447, Arg448, Glu449, Ile556 and Arg557. The former interactions are suggested by the crystallographic data and the latter ones by the predicted binding of the most active naphthyridinone¹⁸ according to our docking method (see [Supplementary data](#)). In order to propose improved structures, we decided to investigate possible substituted analogues of **4a** with our docking protocol. Although simultaneous interactions with His539 and both metallic cofactors do not appear to be possible with our pharmacophore, the introduction of an aromatic side chain at position 8 of our scaffold might thus lead to more potent inhibitors. For instance, a 8-phenethyl, a 8-benzenesulfonamide or a 8-benzamide substituent would be able to occupy the second hydrophobic pocket and greatly improve hydrophobic interactions while maintaining strong metal chelation (see supporting information). Whereas substitutions at position 1 of the heterocyclic scaffold did not yield any promising consistent mode of binding according to our model, an aromatic side chain in position 7 might also be able to fit in this cavity, although it would require more internal ligand strain.

In summary, this novel series of 3-hydroxyquinolin-2(1*H*)-ones was designed to target the magnesium cations within the catalytic core of RT RNase H function. The complexation processes characterized in solution involve the two oxygen atoms of the carbonyl and enolic functions in positions 2 and 3 and docking calculations yielded poses with a consensual binding mode in the RNase H catalytic core. Reproducible inhibitory activities of RT RNase H function with IC₅₀ values around 20 μ M were obtained for a panel of molecules, which mostly includes compounds substituted at position 4 by an amide function. These RNase H inhibitory activities are encouraging since they are close to that of the reference diketoacid, RDS1643. However, they are moderate when compared to other recently reported RNase H inhibitors.^{16–18} Although we clearly demonstrated that 3-hydroxyquinolin-2(1*H*)-ones bind to the RNase H active site, a weak association constant of the magnesium complexes combined with insufficient secondary interactions with proteic residues may provide an explanation for the moderate enzymatic inhibitory properties. The kinetics of the complexation process could have an unfavorable effect as well. By comparing the structures of known potent inhibitors, Kirschberg et al. proposed several structural features for the pharmacophore of RNase H inhibitors.¹⁹ According to them, it must present at least two alcoholic (or phenolic) functions and aromatic electronic forms. Herein our basic scaffold presents two carbonyl and only one alcoholic (enolic) functions. In course of the physicochemical studies, the NMR data of the different ligands alone or complexed with magnesium cations never evidenced any enolization of the cyclic carbonyl function at position 2 of the heterocycle.

We clearly evidenced at least a 12-fold selectivity of these compounds for the RNase H function versus RT polymerase and integrase. This selectivity may be higher since enzymatic assays were only performed at concentrations up to 250 μ M and matches the initial selection criteria of some recently reported thiocarbamates and triazoles.²⁰ Although none of the tested compounds displayed activity in the MT-4 HIV infectivity assay due to limiting cytotoxicity, this should not represent an insurmountable challenge. The CC₅₀ values of our compounds (around 30 μ M) are indeed superior to those of antiviral RNase H inhibitors like naphthyridinones¹⁸ (CC₅₀ = 2–10 μ M) or comparable to those of hydroxytropolones.²¹ One or more reasons which might account for this lack of antiviral activity may be insufficient intrinsic potency, low cell permeability

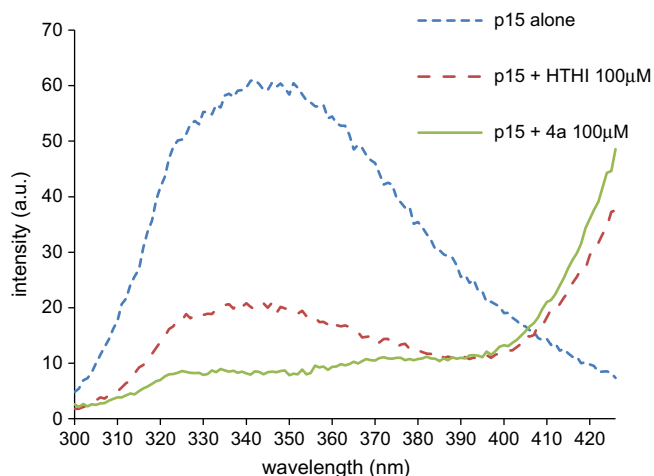


Figure 2. p15 Intrinsic fluorescence quenching assay.

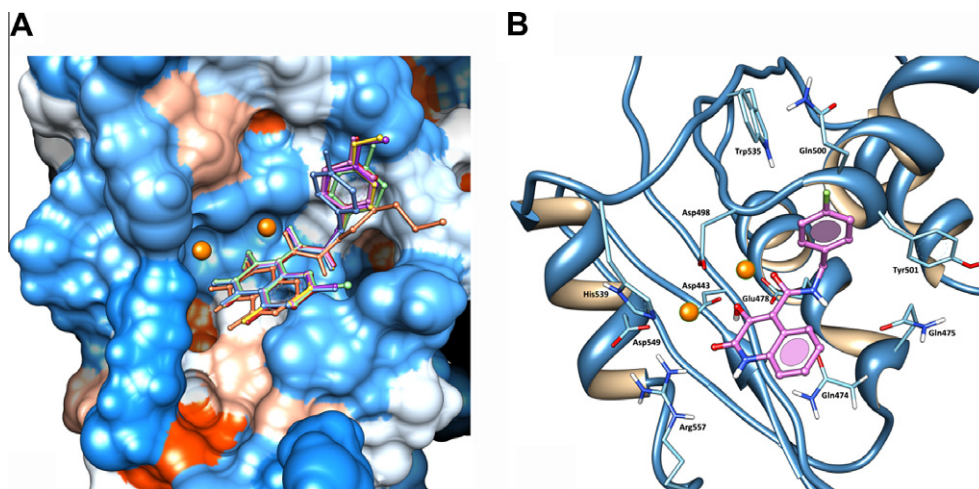


Figure 3. (A): Superimposition of the minimized highest ranked docking solutions of amides **4a** (pink), **4b** (green), **4c** (blue), **4d** (red), **4e** (violet), **4f** (yellow) and **4g** (orange) in the HIV-1 RT RNase H catalytic site. The Connolly isosurface is depicted in blue for the most hydrophilic residues to orange for the most hydrophobic residues. The manganese cofactors are depicted in orange. (B): Putative mode of binding of amide **4a** in the RT RNase H catalytic site.

or high protein binding, and the modest inhibitions of the RNase H function, albeit not solely responsible, indeed represent an important limiting factor. Nevertheless, the encouraging hits of RT RNase H activity on this series of compounds, as well as their selectivity for the HIV-1 RT RNase H site versus the HIV-1 IN and RT polymerase sites, lay the ground for further improvements, and according to our docking studies appropriate substitution of the scaffold by an extended aromatic lipophilic chain might lead to improved activity. Correlating with our molecular docking output, it can be noted that the most potent RNase H inhibitors acting in the submicromolar range all bear bi- or tricyclic (possibly condensed) moieties.^{17–19} The lastly reported work on α -hydroxytropolones illustrates the feasibility of this strategy. Starting from the α -hydroxytropolone manicol, a potent selective but cytotoxic RNase H inhibitor that is ineffective in replication tests, Le Grice and co-workers took advantage from a terminal alkene to synthesize a series of derivatives. Some modified compounds exhibited for the first time antiviral activity at non cytotoxic concentrations.²¹ In this regard, further optimizations of this 3-hydroxyquinolin-2(1H)-one scaffold are currently underway in our laboratories. These studies will be reported in due course.

Acknowledgments

This work was financially supported by le Ministère de l'Enseignement Supérieur et de la Recherche Française and by Fondazione Banco di Sardegna. Francesca Esposito was supported by RAS fellowships, co-financed with funds of PO Sardinia FSE 2007–2013 and of LR 7/2007, projects CRP2_683. Angela Corona was supported by MIUR fellowship DM 198/2003. The Mass Spectrometry facility used in this study was funded by the European Community (FED-ER), the Région Nord-Pas de Calais (France), the CNRS, and the Université des Sciences et Technologies de Lille. We are grateful to Martine Michiels, Nam JooVanderveken, Barbara Van Remoortel and Catherine Meliet for excellent technical assistance.

Supplementary data

Supplementary data associated with this article can be found, in the online version, at <http://dx.doi.org/10.1016/j.bmcl.2012.04.096>.

References and notes

- De Clercq, E. *Curr. Opin. Pharmacol.* **2010**, *10*, 507.
- Mehellou, Y.; De Clercq, E. *J. Med. Chem.* **2010**, *53*, 521.
- Carr, A.; Amin, J. *AIDS* **2009**, *23*, 343.
- Esté, J. A.; Cihlar, T. *Antiviral Res.* **2010**, *85*, 25.
- Tramontano, E. *Mini-Rev. Med. Chem.* **2006**, *6*, 727.
- Tramontano, E.; Di Santo, R. *Curr. Med. Chem.* **2010**, *17*, 2837.
- Tramontano, E.; Esposito, F.; Badas, R.; Di Santo, R.; Costi, R.; La Colla, P. *Antiviral Res.* **2005**, *65*, 117.
- Strashnova, B.; Koval, O. V.; Zaitsev, B. E.; Stash, A. I. *Russ. J. Coord. Chem.* **2008**, *34*, 783.
- Duplantier, A. J.; Becker, S. L.; Bohanon, M. J.; Borzilleri, K. A.; Chrnyk, B. A.; Downs, J. T.; Hu, L. Y.; El-Kattan, A.; James, L. C.; Liu, S.; Lu, J.; Maklad, N.; Mansour, M. N.; Mente, S.; Piotrowski, M. A.; Sakya, S. M.; Sheehan, S.; Steyn, S. J.; Strick, C. A.; Williams, V. A.; Zhang, L. *J. Med. Chem.* **2009**, *52*, 3576.
- Sit, S. Y.; Ehr Gott, F. J.; Gao, J.; Meanwell, N. A. *Bioorg. Med. Chem. Lett.* **1996**, *6*, 499.
- Hang, J. Q.; Rajendran, S.; Yang, Y.; Li, Y.; In, P. W. K.; Overton, H.; Parkes, K. E. B.; Cammack, N.; Martin, J. A.; Klumpp, K. *Biochem. Biophys. Res. Commun.* **2004**, *317*, 321.
- Esposito, F.; Kharlamova, T.; Distinto, S.; Zinzula, L.; Cheng, Y. C.; Dutschman, G.; Floris, G.; Markt, P.; Corona, A.; Tramontano, E. *FEBS J.* **2011**, *278*, 1444.
- Fuji, H.; Urano, E.; Futahashi, Y.; Hamatake, M.; Tatsumi, J.; Hoshino, T.; Morikawa, Y.; Yamamoto, N.; Komano, J. *J. Med. Chem.* **2009**, *52*, 1380.
- Huang, H.; Chopra, R.; Verdine, G.; Harrison, S. *Science* **1998**, *282*, 1669.
- Jones, G.; Willett, P.; Glen, R.; Leach, A.; Taylor, R. *J. Mol. Biol.* **1997**, *267*, 727.
- Billamboz, M.; Bailly, F.; Lion, C.; Touati, N.; Vezin, H.; Calmels, C.; Andréola, M. L.; Christ, F.; Debyser, Z.; Cotellet, P. *J. Med. Chem.* **2011**, *54*, 1812.
- Lansdon, E. B.; Liu, Q.; Leavitt, S. A.; Balakrishnan, M.; Perry, J. K.; Lancaster-Moyer, C.; Kutty, N.; Liu, X.; Squires, N. H.; Watkins, W. J.; Kirschberg, T. A. *Antimicrob. Agents Chemother.* **2011**, *55*, 2905.
- Williams, P. D.; Staas, D. D.; Venkatraman, S.; Loughran, H. M.; Ruzek, R. D.; Booth, T. M.; Lyle, T. A.; Wai, J. S.; Vacca, J. P.; Feuston, B. P.; Ecto, L. T.; Flynn, J. A.; DiStefano, D. J.; Hazuda, D. J.; Bahnck, C. M.; Himmelberger, A. L.; Dornadula, G.; Hrin, R. C.; Stillmock, K. A.; Witmer, M. V.; Miller, M. D.; Grobler, J. A. *Bioorg. Med. Chem. Lett.* **2010**, *20*, 6754.
- Kirschberg, T. A.; Balakrishnan, M.; Squires, N. H.; Barnes, T.; Brenda, K. M.; Chen, X.; Eisenberg, E. J.; Jin, W.; Kutty, N.; Leavitt, S.; Licican, A.; Liu, Q.; Liu, X.; Mak, J.; Perry, J. K.; Wang, M.; Watkins, W. J.; Lansdon, E. B. *J. Med. Chem.* **2009**, *52*, 5781.
- Di Grandi, M.; Olson, M.; Prasad, A. S.; Beberitz, G.; Luckay, A.; Mullen, S.; Hu, Y. B.; Kishnamurthy, G.; Pitts, K.; O'Connell, J. *Bioorg. Med. Chem. Lett.* **2010**, *20*, 398.
- Chung, S.; Himmel, D. M.; Jiang, J. K.; Wojtak, K.; Bauman, J. D.; Rausch, J. W.; Wilson, J. A.; Beutler, J. A.; Thomas, C. J.; Arnold, E.; Le Grice, S. *J. Med. Chem.* **2011**, *54*, 4462.